



A metal-free visible light active photo-electro-Fenton-like cell for organic pollutants degradation

Dongting Yue^a, Xufang Qian^a, Miao Kan^a, Mengyuan Fang^a, Jinping Jia^a, Xudong Yang^b, Yixin Zhao^{a,*}

^a School of Environmental Science and Engineering, Shanghai Jiao Tong University, 800 Dongchuan Road, Shanghai 200240, China

^b State Key Laboratory of Metal Matrix Composites, Shanghai Jiao Tong University, 800 Dong Chuan Road, Minhang District, Shanghai 200240, China



ARTICLE INFO

Keywords:

Visible light
Fenton-like reaction
Mesoporous carbon
g-C₃N₄
Photocatalysts

ABSTRACT

To avoid the potential secondary metal pollution leached from Fenton-like catalysts and use less or no external chemicals supply, we develop an all-carbon based visible light active photo-electro-Fenton-like (PEF) cell to in-situ generate highly active ·OH radical for environmental remediation. In this cell, the mesoporous carbon coated graphite felt (MesoC/GF) cathode could effectively produce H₂O₂ by electrochemical reduction of oxygen. Graphitic carbon nitride (g-C₃N₄) with visible light photocatalytic activities acts as an efficient metal-free Fenton-catalyst for H₂O₂ activation to produce ·OH radical under visible light irradiation. The different cell parameters such as applied voltage, photocatalysts dosage and pH condition have been investigated for phenol removal in aqueous solution. This metal-free visible light active PEF cell shows excellent mineralization efficiency of stubborn phenol with high stability and its performance of phenol removal efficiency is much higher than that of the g-C₃N₄ only photocatalysis cell and MesoC/GF only electrolysis cell. Moreover, our PEF cell presents comparable or even better Fenton-catalytic activities than the similar electro-Fenton cell using MesoC/GF and homogeneous Fe²⁺ ion. These results demonstrate our all-carbon based PEF cell without external chemicals supply is promising for environmental remediation.

1. Introduction

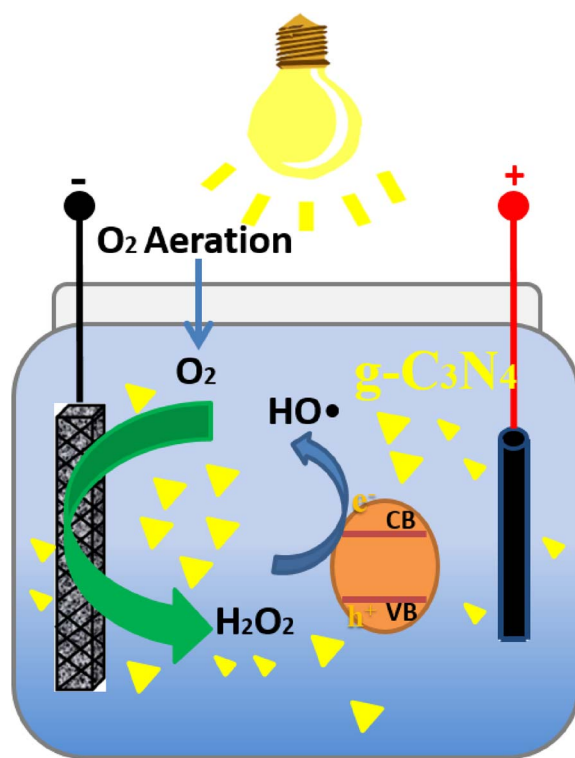
Hydroxyl radical (·OH), as one of the most important reactive oxygen species, has been utilized in various types of environmental remediation including natural waters, the atmosphere, and biological systems [1–5]. With particular attention to its reactivity with various water pollutants, different techniques utilizing hydroxyl radical such as photocatalysis and Fenton reaction have become more and more popular for wastewater treatment [1,6,7]. Recently, advanced oxidation processes based on the generation of ·OH have been regarded as one of the most effective techniques for the mineralization of persist organic contaminants [6–8]. The classical approach for ·OH generation is the regular Fenton reaction using H₂O₂ and Fe²⁺ ion under acidic condition, which is highly active and simple [9]. However, there are two main challenges or problems for homogeneous Fenton reaction: the significant iron residue related secondary pollution and the transportation and storage of H₂O₂ with increased safety regulation [9–12]. To overcome these challenges and problems, it is desired to develop some metal-free methods for in-situ generation of ·OH without external chemicals supply. One promising strategy is to in-situ generate H₂O₂

through electrocatalysis process and then activate the H₂O₂ into ·OH via a Fenton-like catalysts with less or no metal ions leakage [13–16].

Among different cathode candidates for electrochemical H₂O₂ generation, the low cost carbon materials with advantages of non-toxicity, excellent conductivity and good stability are promising for high yield of H₂O₂ [17–19]. The graphite materials such as graphite felt with low cost and high mechanic strength could be a cathode for H₂O₂ generation without any possible metals leaching but exhibited relatively low activities. The mesoporous carbon could improve the efficiency of electrochemical H₂O₂ generation by facilitating the diffusion and storage of oxygen because of its mesoporous structure. However, it is relatively difficult to process into cathodes [20]. In order to achieve the best balance between performance and cost, here we developed an ordered mesoporous carbon (MesoC) coated commercial graphite felt (GF) cathode (noted as MesoC/GF) for H₂O₂ generation via electrochemical reduction of oxygen [20,21]. The catalytic activation of H₂O₂ into ·OH radical is key for Fenton-like reaction, most reported Fenton-like catalysts are based on metal elements to achieve the redox couple for H₂O₂ activation. However, it is so difficult to overcome the metal leaching problem completely when using these metal-based Fenton-like

* Corresponding author.

E-mail address: yixin.Zhao@sjtu.edu.cn (Y. Zhao).



Scheme 1. Schematic illustration of visible light active Photo-Electro-Fenton-like cell based on metal-free carbon materials.

catalysts. Here we adapted a well-known metal-free photocatalyst of $\text{g-C}_3\text{N}_4$ as the visible light active Fenton-like catalyst for activation of H_2O_2 into $\cdot\text{OH}$ [22–32].

Based on these all-carbon materials, we constructed a novel visible light active PEF cell as illustrated in **Scheme 1**. The highly active MesoC/GF cathode could generate H_2O_2 by electrochemical reduction of oxygen, the visible light active $\text{g-C}_3\text{N}_4$ then activates H_2O_2 into $\cdot\text{OH}$. In this PEF cell, issues related to both external chemicals supply and metals leaching can be solved. This configuration not only inherits the advantages of traditional electro-Fenton or photo-Fenton generating the $\cdot\text{OH}$ for the mineralization of most organic pollutant but also has distinct advantages of avoid external chemicals supply and eliminating the metals leaching related environmental risk.

2. Experimental

2.1. Chemicals and reagents

Graphite Felt (GF) was purchased from Jinglongtetan Technology Co. Ltd. Phenol (≥ 99.0 wt %), ethanol, sodium sulfate, iron(III) nitrate nonahydrate, urea, and methanol were purchased from Sinopharm Chemical Reagent Co., Ltd. Sodium hydroxide, hydrochloric acid and hydrogen peroxide (30 wt%) were obtained from Shanghai Lingfeng Chemical Reagent Co., Ltd. Poly (propylene oxide)-blockpoly (ethylene oxide)-block-poly (propylene oxide) triblock copolymer Pluronic F127 ($\text{PEO}_{106}\text{PPO}_{70}\text{PEO}_{106}$, $M_w = 12,600$), 5,5-dimethylpyrrolidine-1-oxide (DMPO) was obtained from Tokyo Chemical Industry Co., Ltd. All the aqueous solutions were prepared by using distilled and deionized water.

2.2. Preparation of MesoC/GF cathode and $\text{g-C}_3\text{N}_4$

MesoC/GF samples were fabricated by a solvent evaporation-induced self-assembly method with copolymer F127 as a template in an ethanol solution. The resol precursor was prepared according to

previous reported methods [33,34]. In a typical preparation, 1.0 g of F127 was first dissolved in 8.0 g ethanol followed by adding 2.0 g 20 wt % resols ethanol solution with stirring for 10 min until forming a homogeneous solution. The commercial GF ($3.0 \text{ cm} \times 3.5 \text{ cm}$) was then soaked in the above solution until saturated. The as-made MesoC/GF samples were then annealed at 350°C for 3 h and 800°C for 2 h under N_2 atmosphere.

$\text{g-C}_3\text{N}_4$ was prepared by a simple thermal polycondensation of urea [25,35]. 10 g urea placed in a crucible with a cover was calcinated at 550°C for 2 h with 4°C min^{-1} heating rate. Once cooling down, the yellowish $\text{g-C}_3\text{N}_4$ was the grinded into powder.

2.3. Characterization

The crystal phase of the samples were using a Shimadzu XRD-6100 diffractometer with $\text{Cu K}\alpha$. The morphological of these samples were characterized by TEM (JEM-2100F) and FESEM (JSM 7800F). Diffuse reflectance spectra (DRS) were measured on a UV-vis spec-trophotometer (Shimadzu UV-2450, Japan). Electron paramagnetic resonance (EPR) spectra was taken on a Bruker EMX-8/2.7C using DMPO as spin trapping agent at 3350 G. The electrochemical test was conducted on CHI 660D electrochemical workstation using the standard Ag/AgCl reference electrode and the graphite counter electrode in 0.05 M Na_2SO_4 solution with 50 mL/min O_2 purging.

2.4. Photo-electro-Fenton-like cell

The $3.0 \text{ cm} \times 3.5 \text{ cm}$ size MesoC/GF acted as the cathode and graphite electrode as the anode in a two-electrode configuration with 50 mL/min O_2 purging under different applied voltages. A 100 W LED lamp (Ceaulight, CEL-LED-100) with double 420 nm cutoff filter was used as light source and the irradiation intensity was 100 mW cm^{-2} . The Photo-Electro-Fenton-like cell contained 70 mL 0.05 M Na_2SO_4 aqueous solution with 50 mg/L phenol as model pollutant and different amount of $\text{g-C}_3\text{N}_4$. The phenol removal samples were taken at given reaction time using $0.45 \mu\text{m}$ membrane filter, and the degradation products and phenol were analyzed on a high-performance liquid chromatography (HPLC, SPD-16, Shimadzu Co., Japan) with a UV-vis detector (270 nm for phenol). Chemical oxygen demand (COD) of the final solution was measured following by China National Standard Method GB11914-89. For the homogeneous system of MesoC/GF electrolysis cell with Fe^{2+} , excess methanol was added into samples that were removed from the cell at specific time intervals for quenching of the reaction. The H_2O_2 concentration was colorimetrically analyzed at 410 nm on the UV spectrophotometer (Cary 60 UV-Vis) using $\text{TiOSO}_4/\text{H}_2\text{SO}_4$ complexation reagent [11,36].

2.5. Results and discussions

The photographs of the commercial GF cathode and the mesoporous carbon modified MesoC/GF cathode are shown in **Fig. 1a**. The MesoC/GF with mesoporous carbon coating looks darker than the bare GF. The SEM image shows that the commercial GF exhibits fiber and belt morphology with a smooth surface, while the surface of MesoC/GF becomes uneven and rough after modified with mesoporous carbon (**Fig. 1b** and c). These mesoporous carbon materials penetrated within the GF frameworks. TEM image of the MesoC/GF in **Fig. 1d** presents the strip like mesopore channels, confirming the ordered hexagonal mesostructure of mesoporous carbon in MesoC/GF cathode [33,37]. These observations are consistent with the fact that the MesoC/GF has a larger BET surface area than the GF (Fig. S1). The electro-catalytic performance of GF and MesoC/GF electrodes for oxygen reduction is presented in **Fig. 1e** and f. The GF electrode shows two reduction peaks at -0.58 V and -1.2 V vs Ag/AgCl. The reduction peaks of MesoC/GF electrode are negatively shifted to -0.42 V and -0.86 V vs Ag/AgCl, respectively. These results demonstrate that MesoC/GF cathode

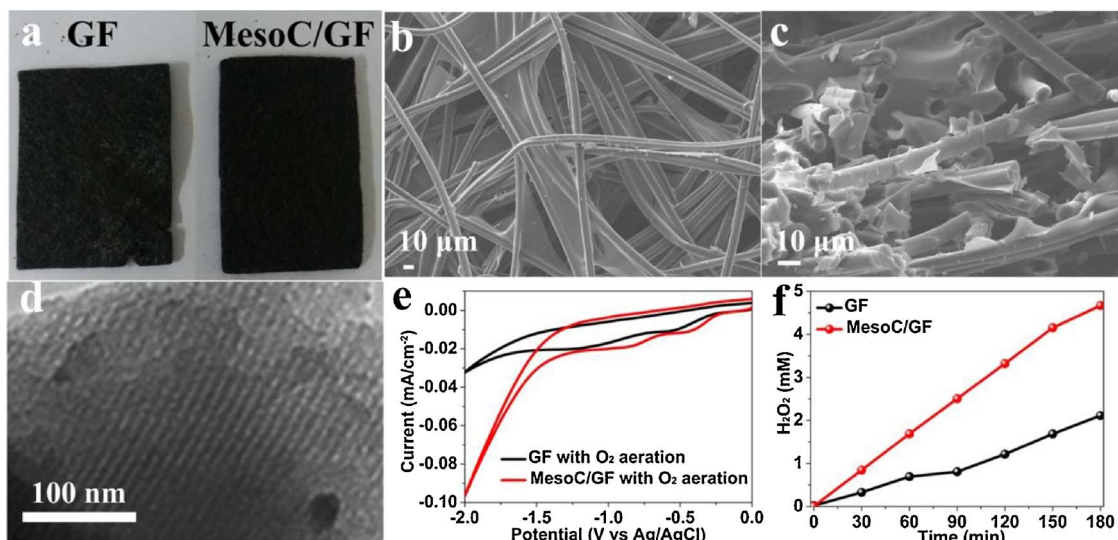


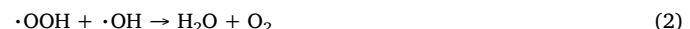
Fig. 1. Photographs (a) and SEM images of GF (b) and MesoC/GF (c), TEM image of MesoC/GF cathode (d), Cyclic voltammograms curve of GF and MesoC/GF cathodes at pH = 3.0 (e), H₂O₂ generation from GF and MesoC/GF cathodes at –0.8 V vs Ag/AgCl and pH = 3.0 (f).

presents the higher electro-catalytic activities for oxygen reduction than GF cathode. Moreover, the rate and amount of H₂O₂ generation by MesoC/GF cathode at –0.8 V vs Ag/AgCl is much higher than GF cathode (Fig. 1f), in which H₂O₂ concentration increases from 2.1 mM to 4.9 mM after 180 min. The modification of commercial GF with MesoC significantly enhanced oxygen reduction activities to generate H₂O₂. It is believed that the introduction of MesoC on GF could facilitate both the electron transfer and the diffusion and storage of oxygen, which would efficiently improve the reduction efficiency of oxygen to produce H₂O₂ on the cathode [38,39]. Consequently, the MesoC/GF cathode is promising for electrochemical generation of H₂O₂.

The metal-free g-C₃N₄ was facilely synthesized and simply grinded as micron size particles, which was easier to separate and recycle than small nanoparticles. XRD patterns of the g-C₃N₄ catalyst presents two distinct diffraction peaks at 13.2° and 27.5°, which is well indexed to g-C₃N₄ (JCPDS Card No.87–1526) (Fig. 2a). The g-C₃N₄ shows an absorption onset edge at ~580 nm in Fig. 2b and the corresponding band gap of the g-C₃N₄ is about 2.7 eV [40–42]. SEM image in Fig. 2c indicates that g-C₃N₄ possesses plate-like structures, which is beneficial for its separation and recycle in real applications. According to previous reports [26,27], the calculated conduction band position of g-C₃N₄ is ~0.88 V vs. NHE, while the valence band is ~2.14 V vs. NHE. Under visible light irradiation, the g-C₃N₄ could generate photoelectrons with potential of ~0.88 V vs. NHE, which have sufficient force to activate H₂O₂ to form ·OH and OH[−]. The energy level diagram for the Fenton activation and the electronic structure of g-C₃N₄ is illustrated in Fig. S2. The products of ·OH and holes are the strong oxidants and could be used for removing organic contaminants.

To simplify the device configuration and reduce instrument cost, we

constructed a two electrodes configuration using a DC power supply to drive electrochemical H₂O₂ generation. The g-C₃N₄ was then suspended in the solution as the photocatalytic Fenton-like catalyst for H₂O₂ activation, as shown in Scheme 1. Under the 1.0 V applied voltage, there is negligible H₂O₂ found in the solution (Fig. 3a) because the applied voltage is not high enough to drive the electrochemical oxygen reduction. Once the applied voltages are increased to 3V and 5V, a large amount of H₂O₂ are generated in the solutions. The stable H₂O₂ concentration could be up to 0.9 mM and 1.6 mM, respectively (Fig. 3a). Here, the H₂O₂ concentration in the PEF cell is lower than the electrolysis only cell because the generated H₂O₂ is consumed by the Fenton-like reaction. The phenol removal efficiency in PEF cell was also investigated with varied parameters. As shown in Fig. 3b, the phenol degradation efficiency by PEF cell was remarkably enhanced with the increase of the applied voltage from 1 V (6.3%) to 3 V (91.1%) when the amount of g-C₃N₄ and phenol was fixed. However, the phenol removal efficiency decreased to 74.2% as the applied voltage was increased to 5 V. This could be due to the variation of H₂O₂ generated at the MesoC/GF cathode at different applied voltages (Fig. 3a). Although the higher amount of H₂O₂ can be generated by MesoC/GF cathode at applied voltage of 5.0 V, the degradation efficiency for phenol at 5.0 V applied voltage decreases and is lower than applied voltage of 3.0 V. This observation could be ascribed to the mechanism that excessive H₂O₂ could act as a self-scavenger for ·OH, following Eqs. (1) and (2), which leads to the greatly decrease of ·OH generation [43].



Here, we fixed the applied voltage as 3 V for electrochemical H₂O₂

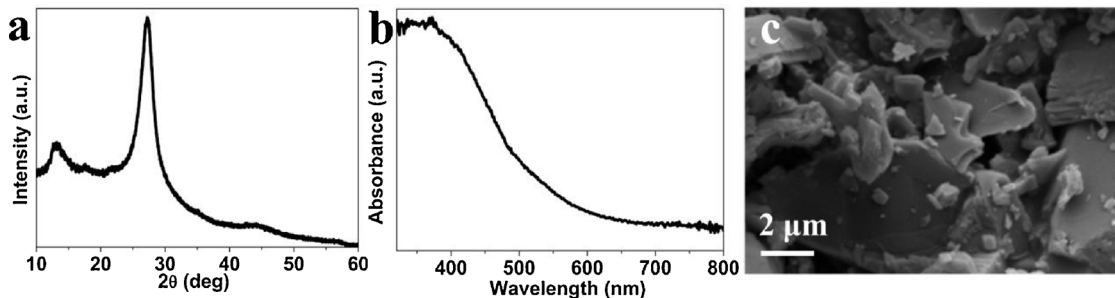


Fig. 2. XRD pattern (a), UV-Vis diffuse reflectance spectrum (b), and SEM images of g-C₃N₄ (c).

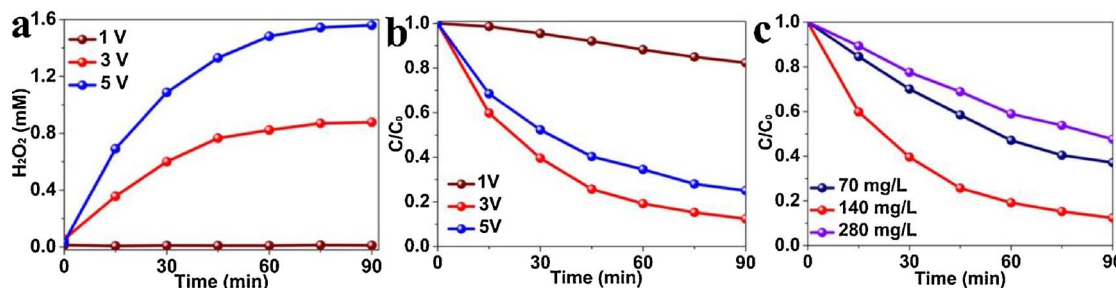


Fig. 3. H₂O₂ generation (a) and phenol degradation (b) in PEF cell at different applied voltage using 140 mg/L g-C₃N₄ at pH = 4.0. The effect of different g-C₃N₄ dosage on phenol degradation with applied voltage 3 V and pH = 4.0 (c).

generation in the following paragraph, the effect of g-C₃N₄ dosage on phenol removal efficiency was also studied. Fig. 3c reveals that the phenol removal efficiency first increases when the dosage of g-C₃N₄ increases from 70 mg/L to 140 mg/L, but then decreases once the amount of g-C₃N₄ increases to 280 mg/L. The decrease of phenol removal efficiency with increase of g-C₃N₄ could be due to the light scattering and light blocking effects by too much g-C₃N₄. Additionally, since some nitrogen-containing by-product may be generated form g-C₃N₄ especially under acidic conditions (pH = 4), leading to the exceeding of total nitrogen concentrations. Total nitrogen (TN) concentrations with different dosage of g-C₃N₄ in phenol solution at pH 3 were investigated in Table S1. These results demonstrated that TN (30.2 mg/L) of 280 mg/L g-C₃N₄ dosage exceeded the standard of TN emission concentration (20.0 mg/L), while TN (14.4 mg/L) of 140 mg/L g-C₃N₄ dosage meet the wastewater regulation. As a result, 140 mg/L of g-C₃N₄ was selected as an optimal photocatalyst dosage for ·OH activation or phenol removal in the following studies. Therefore, the applied voltage of 3.0 V and 140 mg/L g-C₃N₄ was used for the following investigations. The above results have shown that the PEF cell integrating MesoC/GF cathode for in-situ H₂O₂ generation and g-C₃N₄ as visible light active Fenton-like catalyst could effectively degrade phenol using electricity and visible light without external chemicals supply.

To reveal whether the Fenton-like reaction or other mechanism contribute to the phenol degradation, we compare our PEF cell with the g-C₃N₄ only photocatalysis cell and the MesoC/GF only electrolysis cell for degradation of phenol. The MesoC/GF only electrolysis cell with large amounts of H₂O₂ generation presents a lower phenol removal efficiency of 34.8% after 180 min (Fig. 4a). Furthermore, the HPLC results in Fig. 4b revealed that the observed phenol removal was not the complete degradation but only transformation of phenol into some other organic intermediates (Fig. 4b). This result suggested that the H₂O₂ cannot completely degrade phenol but just oxidize it to form some intermediate due to the difficulty of breaking down the benzene ring. In contrast, the phenol removal by g-C₃N₄ only photocatalysis system is just 20.1% but the observed phenol removal is mainly mineralized, which is degraded by the active ·O₂⁻ and h⁺ via the photocatalysis process (Fig. 4b). After coupling the photocatalysis of g-C₃N₄ with MesoC/GF electrolysis cell as PEF cell, the same amount of phenol was rapidly degraded with a removal efficiency of 99.1%. Although most phenol was mineralized into CO₂ and H₂O, some by-product organic compounds including oxalic acid and formic acid were also generated during the degradation process of phenol (Fig. S3). Consequently, a plausible pathways of phenol degradation in the visible active PEF cell was proposed in Fig. S4. Additionally, some other persist organic pollutants including tetracycline and 2,4,6-trichlorophenol were also investigated. Results in Fig. S5 demonstrated that the tetracycline removal efficiency was reached to 90% and complete degradation of 2,4,6-trichlorophenol was achieved within 180 min, suggesting the high activities of PEF cell for persist organic pollutants degradation.

The concentrations of H₂O₂ generated in these different systems were analyzed to explore the different performances of these systems for phenol degradation (Fig. 4c). There was almost no H₂O₂ detected in

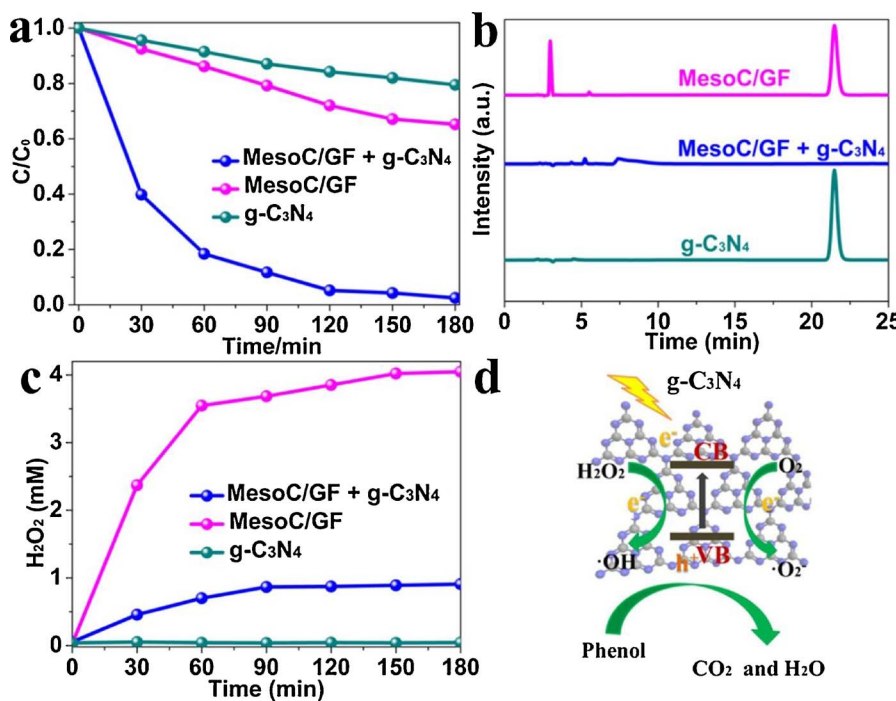
the g-C₃N₄ only photocatalysis, although some previous reports suggested that g-C₃N₄ could produce small amount of H₂O₂ via photocatalysis process. The accumulated H₂O₂ (3.5 mM) in MesoC/GF only electrolysis cell increased rapidly in the first 60 min then grew slowly. The H₂O₂ generated in MesoC/GF only electrolysis cell cannot spontaneously become highly active ·OH, which leads to the lower phenol degradation efficiency with larger amount of H₂O₂. In contrast, the relatively lower concentration of H₂O₂ (0.85 mM) after 60 min in PEF cell was attributed to that most in-situ generated H₂O₂ were effectively converted into ·OH via photogenerated electrons catalytic process. These results are consistent with the above mentioned observation that the phenol removal efficiency via PEF cell is much higher than g-C₃N₄ only photocatalysis cell and MesoC/GF only electrocatalysis cell. Based on above mentioned results, the role of g-C₃N₄ in our PEF cell could not only form the active oxygen species like ·O₂⁻ and highly active h⁺ via the regular photocatalysis process but also produce ·OH by activating in-situ generated H₂O₂, all of which contribute to the high phenol removal efficiency and high mineralization efficiency.

Since the pH values can significantly impact the Fenton reaction, it is necessary to determine the effect of initial pH on the phenol degradation efficiencies (Fig. 5). A notable pH effect was observed in the PEF cell for degradation of phenol. At pH = 3, 99.1% of phenol was degraded within 180 min, while the phenol removal efficiency was 80.2% and 71.3% at pH = 5.0 and 7.0 respectively (Fig. 5a). Simultaneously, the pH variation has no obvious effect on electrochemical generation of H₂O₂ (Fig. 5b). It seems that phenol removal efficiency under different pH values is mainly determined by the activation of ·OH (Eq. (3)) rather than the generation of H₂O₂ (Eq. (4)), although both of which can be affected by pH value. The reason for pH independent electrochemical generation of H₂O₂ in the PEF cell could be that the O₂ diffusion is the limitation reaction step for the O₂ reduction.



The above conclusion was also further confirmed by some control experiments, in which we used the g-C₃N₄ as a photocatalytic Fenton-like catalyst in 0.85 mM H₂O₂ solution containing 50 mg/L phenol. Fig. S6a illustrates that the lower solution pH leads to the enhancement of phenol removal efficiency increases from 18.3% to 40.1%, respectively, within 90 min. Correspondingly, H₂O₂ concentration generally decreases with reaction time, and the amount of H₂O₂ at pH = 3, 5 and 7 is reduced from 0.85 mM to 0.69 mM, 0.76 mM and 0.83 mM, respectively (Fig. S6b). The formation of ·OH catalyzed via photoelectron (Eq. (3)) is facilitated under acidic condition, which is consistent with the highest phenol degradation efficiency at pH = 3. Here the phenol removal efficiency using g-C₃N₄ as photocatalysis with added H₂O₂ is lower than our system incorporated with MesoC/GF for in-situ H₂O₂ generation, which could be ascribed to the factor that the H₂O₂ decreases with reaction and the absence of oxygen bubbling could also reduce the activities of g-C₃N₄.

As shown in Fig. 6a, PEF cell presents the excellent degradation of



phenol over a wide pH range of 3.0–7.0 and the best performance is achieved at pH = 3. The most exciting point is that it is comparable to the traditional Electro-Fenton cell using 2 mg/L Fe²⁺ as H₂O₂ activator when the same MesoC/GF cathode is used as H₂O₂ generator with 3 V applied voltage at pH = 3. The phenol removal efficiency in homogeneous Electro-Fenton cell based on the MesoC/GF electrolysis cell using 2 mg/L Fe²⁺ at neutral pH = 7 decreases to only 30.2%, while our PEF cell still exhibits 72.0% phenol removal. This is a significant enhancement on the phenol removal efficiency under neutral condition by using our PEF cell. The DMPO spin-trapping EPR spectra of our PEF cell is listed in Fig. 6b, which displaces four typical DMPO-OH adducts with intensity of 1:2:2:1 as ·OH. The EPR result confirms the formation of ·OH via Fenton-like photocatalyst of g-C₃N₄ under visible light irradiation. The relative EPR signals intensity decrease at lower pH in both PEF cell and the MesoC/GF electrolysis cell with Fe²⁺. While PEF cell shows much higher intensity of DMPO – OH adduct signal than the case of the MesoC/GF electrolysis cell in the presence of Fe²⁺ at pH = 7. The EPR results are in consistent with the trend of removal efficiency at different pH values, suggesting that the efficient generation of ·OH in PEF cell for the phenol degradation. From the perspective of actual applications, the PEF cell's stability is an important issue that must be considered other than high activities. With the cycle tests, our PEF cell shows almost the same catalytic activity for the phenol decomposition. The COD removal efficiency for all the cycle tests are

Fig. 4. The phenol degradation (a), time-dependent evolution of the HPLC diagrams for phenol degradation after 180 min (b), and the H₂O₂ yield (c) in the different systems: PEF cell based on MesoC/GF + g-C₃N₄, electrolysis cell only based on MesoC/GF, and g-C₃N₄ only photocatalysis cell. Schematic illustration of phenol degradation mechanism in PEF cell based on MesoC/GF + g-C₃N₄ (d).

more than 85% as shown in Fig. 6c and d. To further check the structural stability of g-C₃N₄ catalyst, the crystal structure and morphology of g-C₃N₄ after reaction and annealing treatment were investigated by XRD and SEM. The phase and bulk structure of g-C₃N₄ were maintained similar to those of pristine sample, even the cycle tests (Figure S7 and S8). All these results indicate the high mineralization ability and stability of the PEF cell.

3. Conclusions

In summary, a novel metal-free PEF cell integrating a functional carbon based cathode for H₂O₂ generation with a carbon based photocatalytic Fenton-like catalyst of g-C₃N₄ would not only provide the oxidizing agents including h⁺ and ·O₂^{•-} through the photocatalysis but also in-situ generate ·OH with high activities for environmental remediation. The secondary pollution related to metal residue is completely eliminated in this system. Our work will push forward the application of carbon based cathode materials and visible light driven catalysts for solar energy assisted water treatment and environmental remediation.

Acknowledgement

The authors acknowledge the support of the National Natural

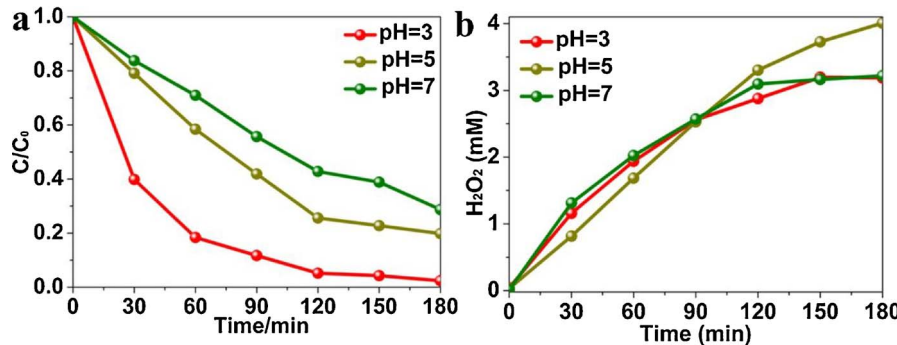


Fig. 5. Phenol degradation by our PEF cell at the different pH with applied voltage 3 V and 140 mg/L g-C₃N₄ (a), Effect of pH on H₂O₂ generation in the absence of g-C₃N₄ (b).

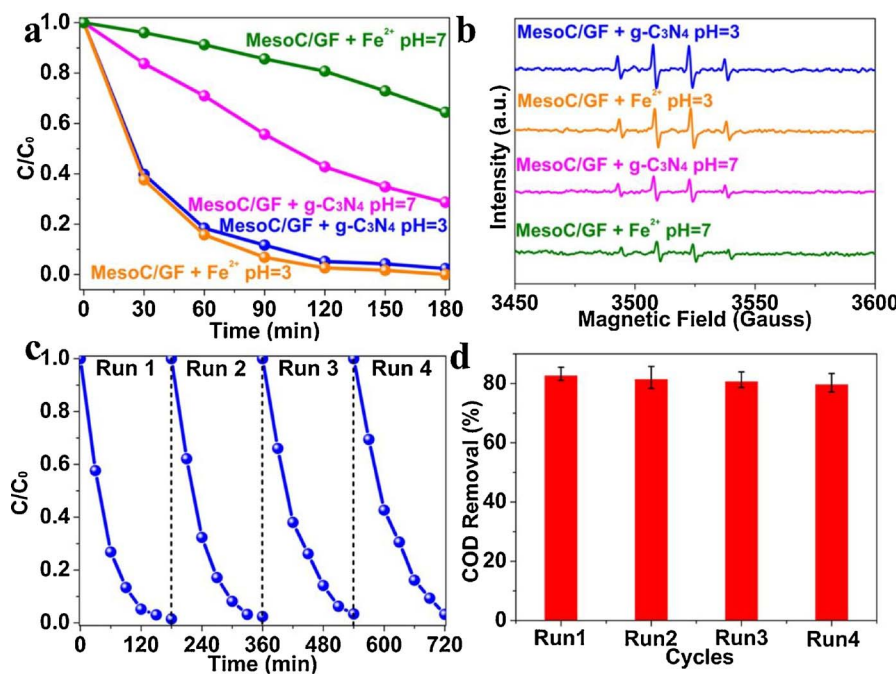


Fig. 6. Effects of pH value on the phenol degradation (a) and DMPO spin-trapping EPR spectra of different pH value on activation (b) via the PEF cell and the MesoC/GF electrolysis cell in the presence of 2 mg/L Fe²⁺. Recycling test of phenol degradation (c) and COD removal efficiency (d) in the PEF cell at pH = 3.0.

Science Foundation of China (Grant No. 21777096 and 21777097) and the China Postdoctoral Science Foundation (Grant No. 2017M621483).

Appendix A. Supplementary data

Supplementary data associated with this article can be found, in the online version, at <https://doi.org/10.1016/j.apcatb.2018.02.033>.

References

- [1] S. Gligorovski, R. Strelkowski, S. Barbuti, D. Vione, Environmental implications of hydroxyl radicals (-OH), *Chem. Rev.* 115 (2015) 13051–13092.
- [2] X.J. Yang, X.M. Xu, J. Xu, Y.F. Han, Iron oxychloride (FeOCl): an efficient Fenton-like catalyst for producing hydroxyl radicals in degradation of organic contaminants, *J. Am. Chem. Soc.* 135 (2013) 16058–16061.
- [3] P.O. Wennberg, Radicals follow the sun, *Nature* 442 (2006) 145–146.
- [4] D. Clifford, D.J. Donaldson, M. Brigante, B. D'Anna, C. George, Reactive uptake of ozone by chlorophyll at aqueous surfaces, *Environ. Sci. Technol.* 42 (2008) 1138–1143.
- [5] F. Rohrer, H. Berresheim, Strong correlation between levels of tropospheric hydroxyl radicals and solar ultraviolet radiation, *Nature* 442 (2006) 184–187.
- [6] M.M. Huber, S. Canonica, G.Y. Park, U.V. Gunten, Oxidation of pharmaceuticals during ozonation and advanced oxidation processes, *Environ. Sci. Technol.* 37 (2003) 1016–1024.
- [7] S. Esplugas, J. Giménez, S. Contreras, E. Pascual, M.R. Guez, Comparison of different advanced oxidation processes for phenol degradation, *Water. Res.* 36 (2002) 1034–1042.
- [8] M. Pera-Titus, V. García-Molina, M.A. Baños, J. Giménez, S. Esplugas, Degradation of chlorophenols by means of advanced oxidation processes: a general review, *Appl. Catal. B-Environ.* 47 (2004) 219–256.
- [9] S. Navalón, M. Alvaro, H. García, Heterogeneous Fenton catalysts based on clays, silicas and zeolites, *Appl. Catal. B-Environ.* 99 (2010) 1–26.
- [10] E. Brillas, I. Sires, M.A. Oturan, Electro-Fenton process and related electrochemical technologies based on Fenton's reaction chemistry, *Chem. Rev.* 109 (2009) 6570–6631.
- [11] X. Qian, M. Ren, Y. Zhu, D. Yue, Y. Han, J. Jia, Y. Zhao, Visible light assisted heterogeneous Fenton-like degradation of organic pollutant via alpha-FeOOH/mesoporous carbon composites, *Environ. Sci. Technol.* 51 (2017) 3993–4000.
- [12] W.D. Oh, Z. Dong, T.T. Lim, Generation of sulfate radical through heterogeneous catalysis for organic contaminants removal: current development, challenges and prospects, *Appl. Catal. B-Environ.* 194 (2016) 169–201.
- [13] Y. Liu, S. Chen, X. Quan, H. Yu, H. Zhao, Y. Zhang, Efficient mineralization of perfluorooctanoate by electro-Fenton with H₂O₂ electro-generated on hierarchically porous carbon, *Environ. Sci. Technol.* 49 (2015) 13528–13533.
- [14] H.Y. Zhao, X.H. Guan, D.L. Wu, G.H. Zhao, Continuous bulk FeCuC aerogel with ultradispersed metal nanoparticles: an efficient 3D heterogeneous electro-Fenton cathode over a wide range of pH 3–9, *Environ. Sci. Technol.* 50 (2016) 5225–5233.
- [15] A. Qian, S. Yuan, P. Zhang, M. Tong, A new mechanism in electrochemical process for arsenic oxidation: production of H₂O₂ from anodic O₂ reduction on the cathode under automatically developed alkaline conditions, *Environ. Sci. Technol.* 49 (2015) 5689–5696.
- [16] M. Sun, X.R. Ru, L.F. Zhai, In-situ fabrication of supported iron oxides from synthetic acid mine drainage: high catalytic activities and good stabilities towards electro-Fenton reaction, *Appl. Catal. B-Environ.* 165 (2015) 103–110.
- [17] J.A. Banuelos, F.J. Rodriguez, J. Manriquez Rocha, E. Bustos, A. Rodriguez, J.C. Cruz, L.G. Arriaga, L.A. Godinez, Novel electro-Fenton approach for regeneration of activated carbon, *Environ. Sci. Technol.* 47 (2013) 7927–7933.
- [18] F. Zhou, C. Lu, Y. Yao, L. Sun, F. Gong, D. Li, K. Pei, W. Lu, W. Chen, Activated carbon fibers as an effective metal-free catalyst for peracetic acid activation: implications for the removal of organic pollutants, *Chem. Eng. J.* 281 (2015) 953–960.
- [19] H. Yano, M. Kataoka, H. Yamashita, H. Uchida, Oxygen reduction activity of carbon-supported Pt-M (M = V, Ni, Cr, Co, and Fe) alloys prepared by nanocapsule method, *Langmuir* 23 (2007) 6438–6445.
- [20] S. Okada, S. Ikuromi, T. Kamegawa, K. Mori, H. Yamashita, Structural design of pd/SiO₂/Ti-containing mesoporous silica core-shell catalyst for efficient one-pot oxidation using in situ produced H₂O₂, *J. Phys. Chem. C* 116 (2012) 14360–14367.
- [21] E. Kan, S.G. Huling, Effects of temperature and acidic pre-treatment on Fenton-driven oxidation of MTBE-spent granular activated carbon, *Environ. Sci. Technol.* 43 (2009) 1493–1499.
- [22] X. Bai, L. Wang, R. Zong, Y. Zhu, Photocatalytic activity enhanced via g-C₃N₄ nanoparticles to nanorods, *J. Phys. Chem. C* 117 (2013) 9952–9961.
- [23] J. Zhang, X. Chen, K. Takanabe, K. Maeda, K. Domen, J.D. Epping, X. Fu, M. Antonietti, X. Wang, Synthesis of a carbon nitride structure for visible-light catalysis by copolymerization, *Angew. Chem. Int. Ed. Engl.* 49 (2010) 441–444.
- [24] J.S. Zhang, J.H. Sun, K. Maeda, K. Domen, P. Liu, M. Antonietti, X.Z. Fu, X.C. Wang, Sulfur-mediated synthesis of carbon nitride: band-gap engineering and improved functions for photocatalysis, *Energy Environ. Sci.* 4 (2011) 675–678.
- [25] Q. Liu, Y. Guo, Z. Chen, Z. Zhang, X. Fang, Constructing a novel ternary Fe(III)/graphene/g-C₃N₄ composite photocatalyst with enhanced visible-light driven photocatalytic activity via interfacial charge transfer effect, *Appl. Catal. B-Environ.* 183 (2016) 231–241.
- [26] J. Liu, Y. Liu, N.Y. Liu, Y.Z. Han, X. Zhang, H. Huang, Y. Lifshitz, S.T. Lee, J. Zhong, Z. Kang, Metal-free efficient photocatalyst for stable visible water splitting via a two-electron pathway, *Science* 347 (2015) 970–974.
- [27] L. Dogliotti, E. Hayon, Flash photolysis of per[oxydi]sulfate ions in aqueous solutions. The sulfate and ozonide radical anions, *J. Phys. Chem. C* 71 (1967) 2511–2516.
- [28] G. Gao, Y. Jiao, F. Ma, Y. Jiao, E. Waclawik, A. Du, Carbon nanodot decorated graphitic carbon nitride: new insights into the enhanced photocatalytic water splitting from ab initio studies, *Phys. Chem. Chem. Phys.* 17 (2015) 31140–31144.
- [29] J. Ran, T.Y. Ma, G. Gao, X.-W. Du, S.Z. Qiao, Porous P-doped graphitic carbon nitride nanosheets for synergistically enhanced visible-light photocatalytic H₂ production, *Energy Environ. Sci.* 8 (2015) 3708–3717.
- [30] G. Li, Z. Lian, W. Wang, D. Zhang, H. Li, Nanotube-confinement induced size-controllable g-C₃N₄ quantum dots modified single-crystalline TiO₂ nanotube arrays for stable synergistic photoelectrocatalysis, *Nano Energy* 19 (2016) 446–454.
- [31] G. Li, X. Nie, J. Chen, Q. Jiang, T. An, P.K. Wong, H. Zhao, H. Yamashita,

- Enhanced visible-light-driven photocatalytic inactivation of Escherichia coli using g-C₃N₄/TiO₂ hybrid photocatalyst synthesized using a hydrothermal-calcination approach, *Water. Res.* 86 (2015) 17–24.
- [32] C. Pan, J. Xu, Y. Wang, D. Li, Y. Zhu, Dramatic activity of C₃N₄/BiPO₄ photocatalyst with core/shell structure formed by self-assembly, *Adv. Funct. Mater.* 22 (2012) 1518–1524.
- [33] R.L. Liu, Y.F. Shi, Y. Wan, Y. Meng, F.Q. Zhang, D. Gu, Z.X. Chen, B. Tu, D. Zhao, Triconstituent Co-assembly to ordered mesostructured polymer-silica and carbon-silica nanocomposites and large-pore mesoporous carbons with high surface areas, *J. Am. Chem. Soc.* 128 (2006) 11652–11662.
- [34] Y. Meng, D. Gu, F.Q. Zhang, Y.F. Shi, H.F. Yang, Z. Li, C.Z. Yu, B. Tu, D.Y. Zhao, Ordered mesoporous polymers and homologous carbon frameworks: amphiphilic surfactant templating and direct transformation, *Angew. Chem. Int. Ed. Engl.* 44 (2005) 7053–7059.
- [35] Z. Chen, P. Sun, B. Fan, Z. Zhang, X. Fang, In situ template-free ion-exchange process to prepare visible-light-active g-C₃N₄/NiS hybrid photocatalysts with enhanced hydrogen evolution activity, *J. Phys. Chem. C* 118 (2014) 7801–7807.
- [36] X.J. Yang, P.F. Tian, H.L. Wang, J. Xu, Y.F. Han, Catalytic decomposition of H₂O₂ over a Au/carbon catalyst: A dual intermediate model for the generation of hydroxyl radicals, *J. Catal.* 336 (2016) 126–132.
- [37] Y. Wang, H. Zhao, G. Zhao, Iron-copper bimetallic nanoparticles embedded within ordered mesoporous carbon as effective and stable heterogeneous Fenton catalyst for the degradation of organic contaminants, *Appl. Catal. B-Environ.* 164 (2015) 396–406.
- [38] X. Guo, D. Li, J. Wan, X. Yu, Preparation and electrochemical property of TiO₂/nano-graphite composite anode for electro-catalytic degradation of ceftriaxone sodium, *Electrochim. Acta* 180 (2015) 957–964.
- [39] Y. Lin, J. Yu, Z. Xing, X. Guo, X. Yu, B. Tang, J. Zou, Enhanced generation of H₂O₂ and radicals on Co₉S₈/partly-graphitized carbon cathode for degradation of bio-refractory organic wastewater, *Electrochim. Acta* 213 (2016) 341–350.
- [40] Y. Yang, Y. Guo, F. Liu, X. Yuan, Y. Guo, S. Zhang, W. Guo, M. Huo, Preparation and enhanced visible-light photocatalytic activity of silver deposited graphitic carbon nitride plasmonic photocatalyst, *Appl. Catal. B-Environ.* 142–143 (2013) 828–837.
- [41] X. Wang, K. Maeda, A. Thomas, K. Takanabe, G. Xin, J.M. Carlsson, K. Domen, M. Antonietti, A metal-free polymeric photocatalyst for hydrogen production from water under visible light, *Nat. Mater.* 8 (2009) 76–80.
- [42] X. Wang, S. Blechert, M. Antonietti, Polymeric graphitic carbon nitride for heterogeneous photocatalysis, *ACS Catal.* 2 (2012) 1596–1606.
- [43] T. Watanabe, T. Takirawa, K. Honda, Photocatalysis through excitation of adsorbates. 1. Highly efficient N-deethylation of rhodamine B adsorbed to CdS, *J. Phys. Chem.* 81 (2018) 1845–1851.